JOURNAL OF GEOPHYSICAL RESEARCH, VOL. 117, D12111, doi:10.1029/2011JD017385, 2012

The relationship between El Niño and the western North Pacific summer climate in a coupled GCM: Role of the transition of El Niño decaying phases

Wei Chen,[1] Jong-Kil Park,[2] Buwen Dong,[3] Riyu Lu,[1] and Woo-Sik Jung[2]

Received 21 December 2011; revised 18 May 2012; accepted 21 May 2012; published 29 June 2012.

[1] This study investigates the impacts of the transition of El Niño decaying phases on the western North Pacific anticyclone (WNPAC) anomalies in the subsequent summer with a coupled GCM. The modeling results suggest that the El Niños with short decaying phases lead to significant WNPAC anomalies in the following summer, which are contributed to mainly by the El Niños followed by La Niñas, in comparison with those not followed by La Niñas. In contrast, the long decaying cases are associated with the disappearance of WNPAC anomalies in the summer. These differences in the WNP circulation anomalies can be explained by the different configurations of simultaneous SSTs in the Indian Ocean and in the central and eastern tropical Pacific: positive SSTs in the former region and negative ones in the latter region constructively induce significant WNPAC anomalies for the short decaying cases, while the roles of positive SSTs in both regions for the long decaying cases work destructively and lead to weak WNP circulation anomalies. Further analysis indicates that the different lengths of El Niño decaying phases are predicted by the strength of Indian Ocean SSTs in the mature winter. The warmer wintertime Indian Ocean SSTs favor the anomalous easterly wind over the western and central equatorial Pacific in the subsequent summer, leading to a short decaying of El Niño. Thus, the strength of wintertime Indian Ocean SSTs is one of the important factors that affect the length of El Niño decaying phase and resultant WNPAC anomalies in the following summer.

Citation: Chen, W., J.-K. Park, B. Dong, R. Lu, and W.-S. Jung (2012), The relationship between El Niño and the western North Pacific summer climate in a coupled GCM: Role of the transition of El Niño decaying phases, *J. Geophys. Res.*, *117*, D12111, doi:10.1029/2011JD017385.

1. Introduction

[2] The western North Pacific (WNP) summer climate is one of the important subcomponents of the Asian summer monsoon. The convective activity over the WNP region displays pronounced interannual variability and has considerable impacts on the climate over East Asia [e.g., *Nitta*, 1987]. El Niño – Southern Oscillation (ENSO) has been recognized as the primary factor which determines the interannual variability of the summer climate over the WNP and East Asia [e.g., *Chang et al.*, 2000; *Chou et al.*, 2009; *Lin and Lu*, 2009]. The climatic anomalies over the WNP are related to different phases of ENSO [e.g., *Chou et al.*, 2003; *Wang et al.*, 2003; *Hu and Huang*, 2010]. Precipitation anomalies over the WNP tend to be positive during El Niño developing years and negative during El Niño decaying years [*Chou et al.*, 2003].

[3] The impacts of ENSO on the climate over the WNP region during its decaying summers attract more attention because of the significant signals and predictability of the WNP summer anomalies. Western North Pacific anticyclonic (WNPAC) anomalies, emerging in the El Niño mature winter and maintaining during the following spring and summer, are the crucial components in reflecting the relationship between El Niño and the WNP summer climate in the El Niño decaying summer [e.g., *Zhang et al.*, 1999; *Lau and Nath*, 2000; *Zhang and Sumi*, 2002; *Chou et al.*, 2003; *Wang et al.*, 2003].

[4] The variations of the WNPAC anomalies are associated with differences in ENSO activity. The increased magnitude and periodicity of ENSO induce strengthened monsoon – ocean interaction over the WNP region, which makes the WNPAC anomalies last longer during the El Niño decaying summer [*Wang et al.*, 2008], and influences the precipitation pattern over East Asia [*Xue and Liu*, 2008]. The increased ENSO amplitude also causes the enhancement

[1]State Key Laboratory of Numerical Modelling for Atmospheric Sciences and Geophysical Fluid Dynamics, Institute of Atmospheric Physics, Chinese Academy of Sciences, Beijing, China.
[2]Department of Atmospheric Environment Information Engineering, Atmospheric Environment Information Research Center, Inje University, Gimhae, South Korea.
[3]National Centre for Atmospheric Science, Department of Meteorology, University of Reading, Reading, UK.

Corresponding author: W. Chen, State Key Laboratory of Numerical Modelling for Atmospheric Sciences and Geophysical Fluid Dynamics, Institute of Atmospheric Physics, Chinese Academy of Sciences, PO Box 9804, Beijing 100029, China. (chenwei@mail.iap.ac.cn)

0148-0227/12/2011JD017385

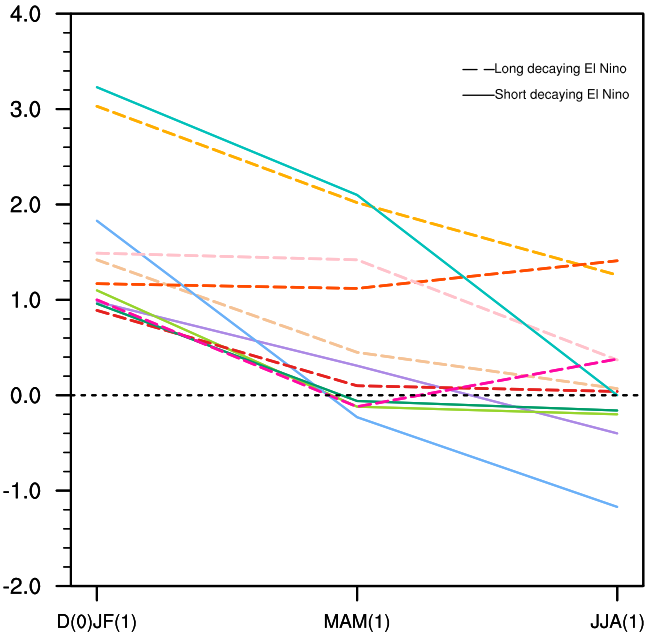

Figure 1. Seasonal evolution of the Niño 3 index (units: °C) associated with the 11 El Niño events in observations. The winters corresponding to the selected El Niño events are designated as D(0)JF(1), and the years preceding and following these events are designated as Year(0) and Year(1), respectively. The solid colored lines represent the El Niño events with short decaying phases (JJA(1) Niño 3 index is negative), and the dashed colored lines represent the Niño events with long decaying phases (JJA(1) Niño 3 index is positive).

of the air–sea interaction in the Indian Ocean. The positive SST anomalies in the Indian Ocean, following the wintertime El Niño events, contribute to the reinforcement of the WNPAC anomalies [*Watanabe and Jin*, 2002; *Terao and Kubota*, 2005; *Yang et al.*, 2007; *Li et al.*, 2008; *Ding et al.*, 2010; *Xie et al.*, 2009]. In addition, coupled model results suggested that strong El Niño events, tending to be followed by short decaying phases, are in favor of the maintenance of the WNPAC anomalies from subsequent spring to summer [*Li et al.*, 2007].

[5] As an important feature of El Niño, the persistence of decaying phases, however, varies from case to case. This can be illustrated by the seasonal evolutions of El Niño events (Figure 1). Here, a warm event is defined when the DJF (December–January–February)-mean Niño 3 index (defined as the SST anomalies averaged over 5°S–5°N, 150–90°W) is larger than 0.8 standard deviation from the time mean. Under this criterion, the years 1951/52, 1957/58, 1965/66, 1972/73, 1976/77, 1982/83, 1986/87, 1991/92, 1994/95, 1997/98 and 2002/03 are chosen as 11 El Niño events from observations. Figure 1 shows that some El Niño events are followed by short decaying phases while other cases are followed by long decaying phases. This difference in the length of decaying phase leads to a wide spread among Niño 3 index values in the decaying summer JJA(1): the standard deviation of JJA(1) Niño 3 index values among the 11 cases is 0.72°C, which is comparable to that of the D(0)JF(1) Niño 3 index (0.83°C).

[6] Figure 1 hints that the impacts of El Niño in the mature winter on the following summer climatic anomalies over the WNP might depend on two features of El Niño: the intensity of wintertime El Niño and the length of the decaying phase. Some previous studies have indicated that these two features are related to each other, i.e., strong El Niño events tend to be followed by short decaying phases [*Boo et al.*, 2004; *Kug and Kang*, 2006; *Li et al.*, 2007]. *Li et al.* [2007] suggested that strong El Niño events, being followed by short decaying phases, result in strong WNPAC anomalies in the summer. However, they did not separately evaluate the roles of wintertime intensity and the decaying phase of El Niño events. In this study, we attempt to assess the relative roles of these two features in affecting the WNP summer climatic anomalies. Since the observational record is too short and there are not enough events to be used to address this question, we turn to analyze the simulation results by a coupled atmosphere–ocean model and check the main conclusion by observational analysis.

[7] The rest of the paper is organized as follows. After a brief description of the model and data set in Section 2, the model results are analyzed in Sections 3 and 4: roles of the El Niño decaying phases in the relationship between El Niño and the WNP summer climate are illustrated in Section 3, and the impacts of El Niño intensity on the WNPAC anomalies are demonstrated by removing the influence of decaying phases in Section 4. In addition, observational evidence of the impacts of El Niño decaying phases is investigated in Section 5. Finally, a discussion and conclusions are presented in Section 6.

2. Model and Experiment

[8] The model used in this study is a coupled atmosphere-ocean GCM developed by the Hadley Centre, named as HadCM3. The atmospheric component of HadCM3 has 19 levels with a horizontal resolution of 2.5° of latitude by 3.75° of longitude [*Pope et al.*, 2000], and the oceanic component has 20 levels with a horizontal resolution of 1.25° by 1.25°. The coupled model run uses constant pre-industrial trace gas concentrations and incoming solar radiation. The model has been integrated without flux adjustment for over 1000 years with stable climate [*Gordon et al.*, 2000]. A 1000-year simulation of this pre-industrial run is analyzed in this study.

[9] The observational data used here are reconstructed monthly mean SST from 1948 to 2003 [*Smith and Reynolds*, 2004], and monthly mean NECP/NCAR reanalysis data for the same period [*Kalnay et al.*, 1996].

[10] One hundred and fifty-two El Niño events are yielded in the 1000-year pre-industrial simulation, which are defined as the DJF-mean Niño 3 index being larger than one standard deviation from the time mean. This criterion is similar to that used in observations. Figure 2 shows the composite seasonal evolution of El Niño events both in the model and observations. The model basically reproduces the amplitude, growth and decay of the warm events [e.g., *Li et al.*, 2007]. The positive SST anomalies develop around the preceding spring, labeled as MAM(0), grow over the next two seasons and reach their peak in the winter D(0)JF(1). After the mature winter, the positive SST anomalies weaken in the following spring MAM(1), and transfer to a normal state in

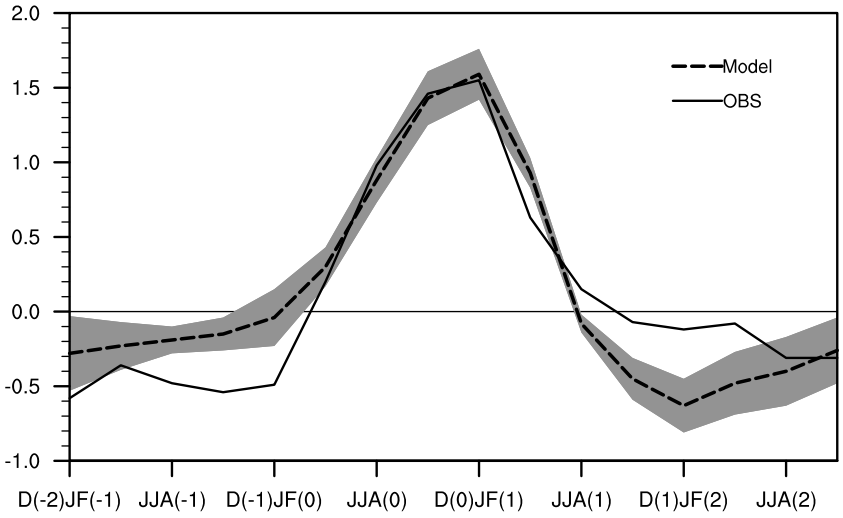

Figure 2. Composite evolution of the Niño 3 index for El Niño events in observations (solid line), and in the model simulation (dashed line). The shading indicates one standard deviation by using 100-year chunks in the 1000-year pre-industrial simulation.

the summer JJA(1). These features are consistent with the composite of 11 El Niño events in observations.

[11] *Li et al.* [2007] evaluated the model's ability in simulating the anomalous anticyclones over the WNP and the south Indian Ocean associated with the different phases of ENSO. They suggested that the HadCM3 coupled model reproduces the climatological distribution of 850-hPa wind over the WNP and precipitation in the tropical Pacific. Furthermore, the model captures the basic features of the WNPAC anomalies associated with ENSO phases: the WNPAC anomalies form in the previous autumn SON(0), reach their peak during the El Niño mature winter D(0)JF(1) and the following spring MAM(1), and decay rapidly in the subsequent summer JJA(1). Thus, the results simulated by this model can be used to analyze the impacts of El Niño behavior on the WNP summer climate.

3. Roles of the El Niño Decaying Phases in the Relationship Between El Niño and WNP Summer Climate

3.1. Impacts of the Length of El Niño Decaying Phases

[12] The 152 El Niño events in the 1000-year pre-industrial simulation are divided into two categories: short decaying and long decaying El Niño cases. The El Niño events for which the JJA(1) Niño 3 index is less (greater) than 0°C are classified as the short (long) decaying events. This criterion yields 84 short decaying and 68 long decaying El Niño cases.

[13] Figure 3 depicts the seasonal evolution of the Niño 3 index for the composite short and long decaying cases, respectively. These two kinds of El Niño both develop around the spring MAM(0) and peak in the winter D(0)JF(1) with similar strength. However, after the mature winter, the positive SST anomalies in the eastern tropical Pacific decline faster and transform to negative SST anomalies in the summer JJA(1) for the short decaying events. On the other hand, the positive SST anomalies for the long decaying events maintain until the next winter D(1)JF(2). During the El Niño decaying summer JJA(1), the strength of the Niño 3 index is about 0.8°C for the long decaying events, which contrast sharply with −0.7°C for the short decaying ones. In addition, Figure 3 also implies that El Niño events with similar intensity can be followed by different decaying phases.

[14] The composite stream function anomalies for the short and long decaying events are shown in Figure 4. The significant WNPAC anomalies associated with the short decaying cases (Figure 4c) in JJA(1) suggest that there is a significant relationship between short decaying El Niño events and -WNP summer climate. The center of the WNPAC anomalies in the mature winter D(0)JF(1) and following spring MAM(1) are located in the South China Sea, showing a slight- eastward shift with time, which is in agreement with previous studies [e.g., *Wang et al.*, 2003; *Li et al.*, 2007]. For the long decaying events, the WNPAC anomalies in D(0)JF(1) and MAM(1) are roughly similar to those for the short decaying events. Although the WNPAC anomalies are weaker than those for short decaying events in D(0)JF(1) (Figures 4a and 4d), they are very similar in MAM(1) (Figures 4b and 4e).

[15] The most remarkable difference of the WNPAC anomalies between the short and long decaying events appears in JJA(1) (Figures 4c and 4f). The significant WNPAC anomalies persist for the short decaying cases, while they disappear and even weak cyclonic anomalies emerge over the WNP region for the long decaying cases. This pronounced difference suggests that the El Niño events with short decaying phases, rather than with long decaying phases, have strong impacts on the WNP summer climate.

[16] In addition, a pair of cyclonic circulation anomalies over the central and eastern Pacific is found for both the short and long decaying cases, but the intensity is quite different. The strength of these cyclonic anomalies for the long decaying events is roughly twice that of the short decaying cases in D(0)JF(1) and MAM(1). This implies that the anomalous westerly flow over the central and eastern equatorial Pacific is stronger for the long decaying cases, which favors the persistence of positive SST anomalies in

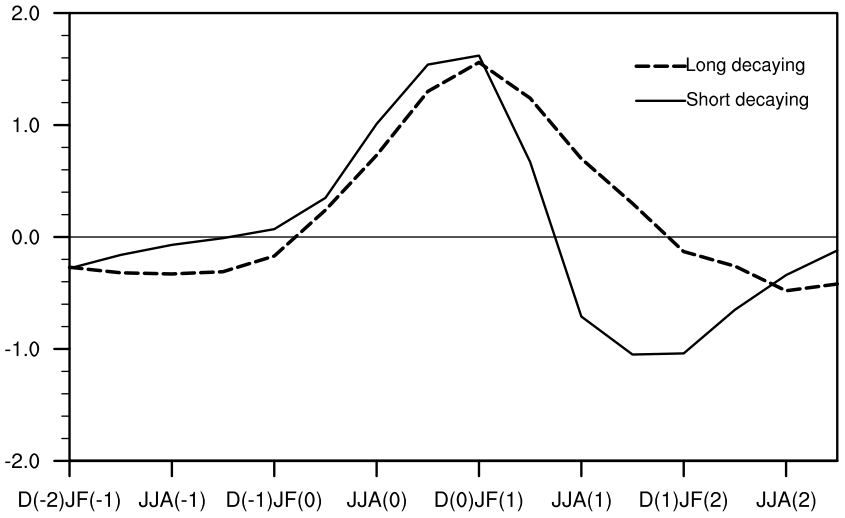

Figure 3. Composite evolution of the Niño 3 index for the short decaying El Niño events (solid line) and for the long decaying ones (dashed line) in the 1000-year pre-industrial simulation. The short (long) decaying El Niño events are defined by the Niño 3 index in the decaying summer JJA(1) being less (greater) than 0°C.

the central and eastern tropical Pacific by suppressing the upwelling there.

[17] The El Niño-related SST anomalies for the short and long decaying events are shown in Figure 5. The different strengths of SST anomalies over the Indian Ocean in the mature winter are related to different lengths of decaying phases, even though the SST anomalies in the central and eastern tropical Pacific are similar for the two categories of El Niño. The correlation coefficient between the D(0)JF(1) Indian Ocean SST anomalies averaged over the region (10°S–20°N, 40–110°E) and the JJA(1) Niño 3 index is −0.48, which indicates that the strong positive Indian Ocean SST anomalies in the mature winter are associated with the strong negative SST anomalies over the central and eastern tropical Pacific in the decaying summer. In D(0)JF(1), the Indian Ocean SST anomalies are significantly positive, with the regional averaged value of 0.42°C for the short decaying cases. Conversely, they are weak (with regional averaged value of 0.22) for the long decaying El Niño events. The impacts of wintertime Indian Ocean SST anomalies on the decline of El Niño have been proposed by *Annamalai et al.* [2005, 2010], *Kug and Kang* [2006] and *Ohba and Ueda* [2007]. Collectively, the work reported by these authors suggested that the strong positive Indian Ocean SST anomalies generate the easterly flow extending to the western equatorial Pacific by inducing an atmospheric Kelvin wave, which can be detected by the strong WNPAC anomalies in D(0)JF(1) (Figure 4a). During MAM(1), the anomalous easterly flow is enhanced and expanded to the central and eastern equatorial Pacific, which weakens the cyclonic circulation in the central and eastern Pacific (Figure 4b), and leads to a decline of positive SST anomalies in the eastern tropical Pacific (Figure 5b). In JJA(1), the positive SST anomalies in the central and eastern tropical Pacific transform into negative anomalies, which indicates the rapid- decline of El Niño events. This short maintenance of the El Niño decaying phase is contributed to by the anomalous easterly flow over the equatorial Pacific, induced by the significantly positive Indian Ocean SST anomalies in the mature winter.

[18] Unlike the short decaying cases, in D(0)JF(1), the Indian Ocean SST anomalies are insignificant for the long decaying El Niño events (Figure 5d), even though they both have similar strength SST anomalies in the central and eastern tropical Pacific. The insignificant Indian Ocean SST anomalies hardly influence the wind anomalies over the equatorial Pacific, so the WNPAC anomalies are weaker in D(0)JF(1) and the cyclonic anomalies in the central and eastern Pacific are stronger in MAM(1) than those for short decaying cases. The strong westerly flow over the central and eastern equatorial Pacific associated with the strong cyclonic circulation weakens the easterly trade winds and leads to a long decaying of El Niño. Thus the positive SST anomalies in the central and eastern tropical Pacific still persist in JJA(1) (Figure 5f). The SST anomalies over the Indian Ocean in the mature winter affect the length of El Niño decaying phase through modifying the wind anomalies over the equatorial Pacific. The wintertime intensity of Indian Ocean SST anomalies is a precursor to the different lengths of El Niño decaying phases. It should be mentioned that the different Indian Ocean SST anomalies in the mature winter corresponding to the short and long decaying cases are related to the similar strength of wintertime El Niño. This implies that the warming in the Indian Ocean is not only a part of the El Niño signal [e.g., *Lau and Nath*, 2000; *Kug and Kang*, 2006], but also relates to the dynamic processes over the Indian Ocean [*Ueda and Matsumoto*, 2000; *Xie et al.*, 2002; *Lau and Nath*, 2003].

[19] Furthermore, the circulation anomalies over the WNP in the El Niño decaying summer JJA(1) for the short and long decaying cases are related to the simultaneous SST anomalies. For the short decaying cases, the strong WNPAC anomalies shown in Figure 4c are associated with the configurations of SST anomalies in the Indian Ocean and in the central and eastern tropical Pacific (Figure 5c). On the one hand, the negative SST anomalies in the central and eastern tropical Pacific are in favor of a pair of anticyclonic circulation anomalies on the western side according to the Gill's

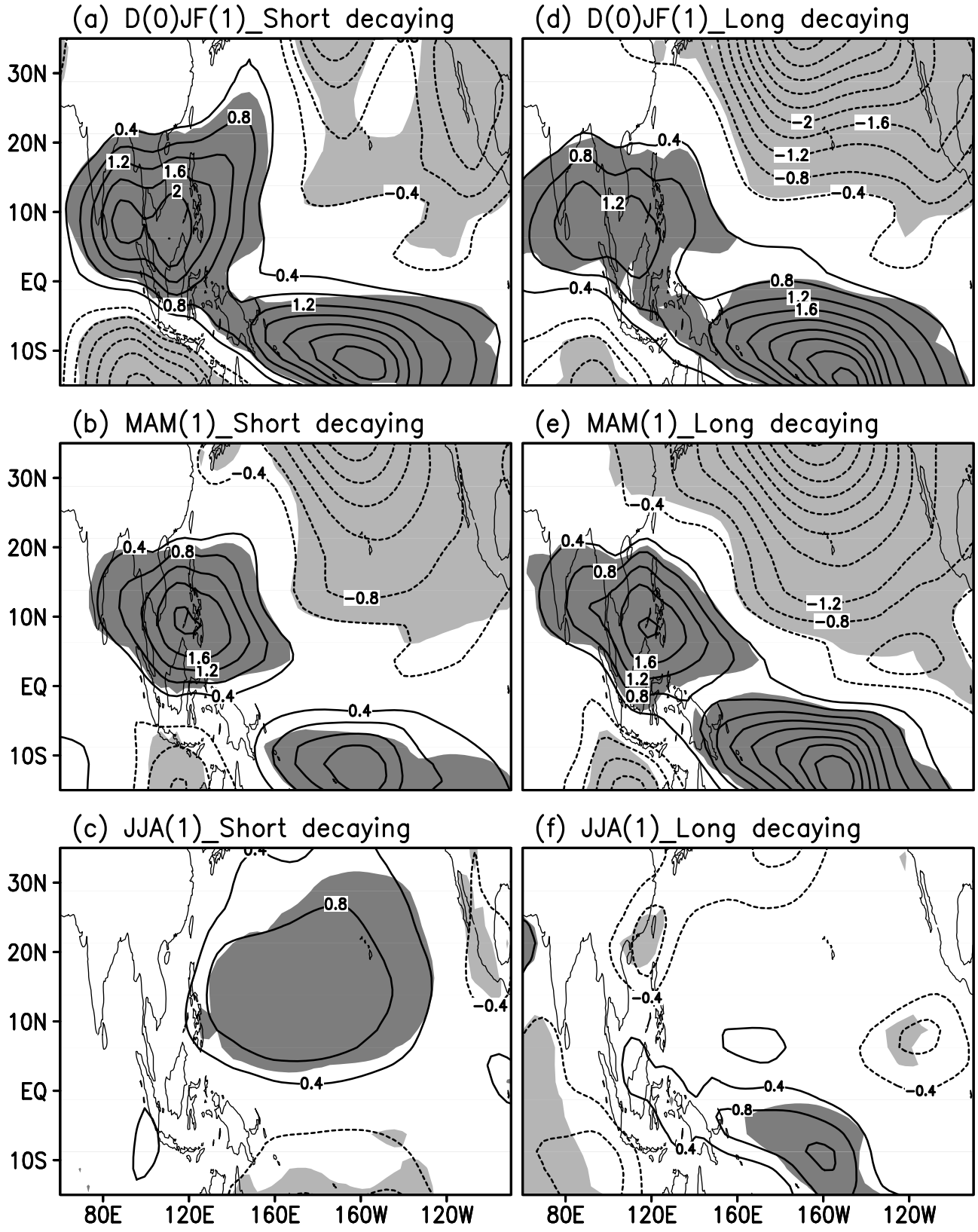

Figure 4. Composite 850-hPa stream function anomalies (units: 10^6 m^2 s^{-1}) for (a–c) the short decaying El Niño events and (d–f) the long decaying ones from El Niño peak winter D(0)JF(1) to the decaying summer JJA(1). Shading indicates the region where the differences are significant at the 95% confidence level by *t*-test.

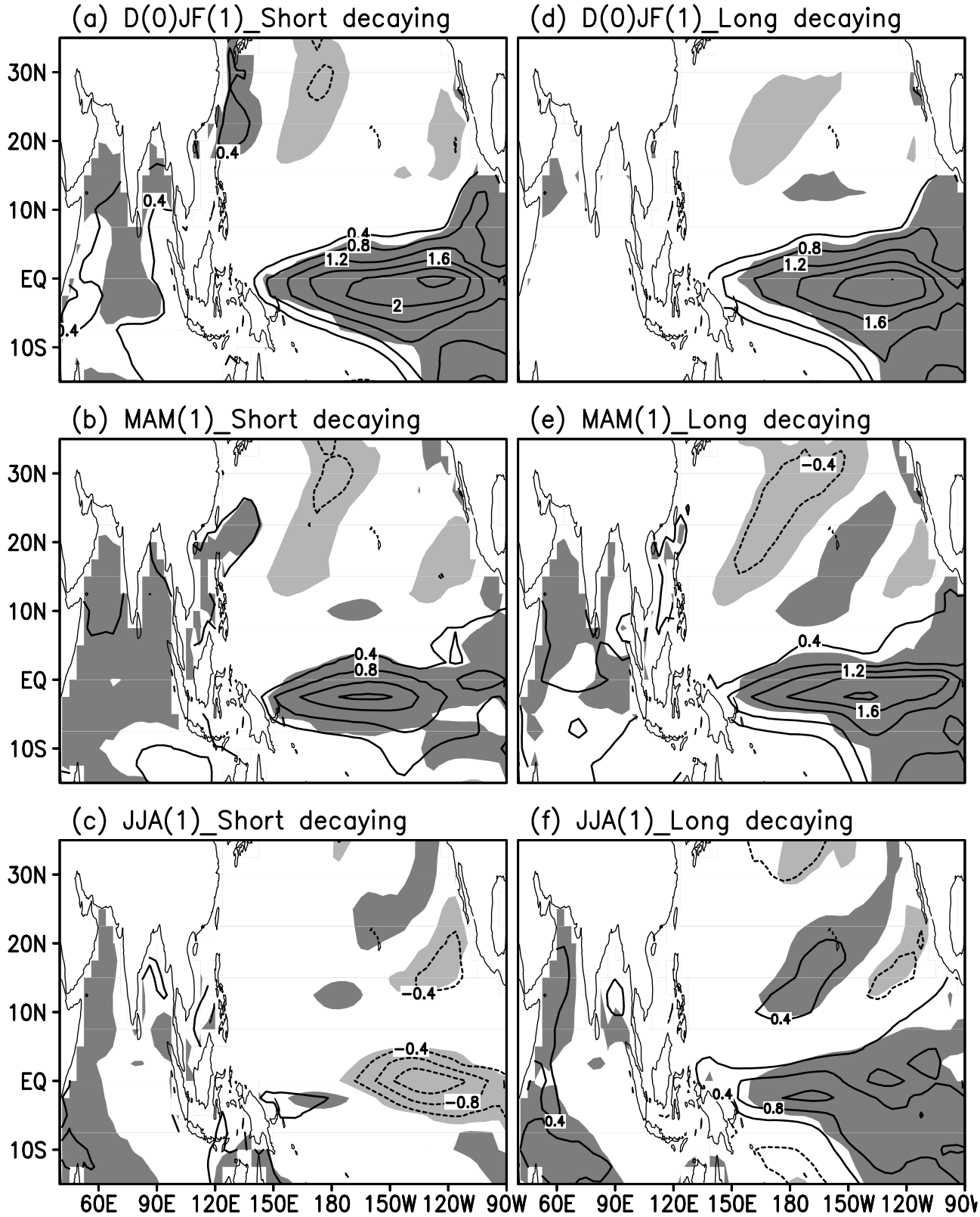

Figure 5. As in Figure 4, but for SST anomalies (units: °C).

theoretical model; but on the other hand, previous studies have indicated that the positive SST anomalies in the Indian Ocean contribute to the persistence of the WNPAC anomalies [e.g., *Yang et al.*, 2007; *Li et al.*, 2008]. *Xie et al.* [2009] suggested that the warm SSTs in the Indian Ocean excite a warm Kelvin wave into the western Pacific, inducing surface wind divergence and suppressing convection over the WNP region, therefore strengthening the WNPAC anomalies in

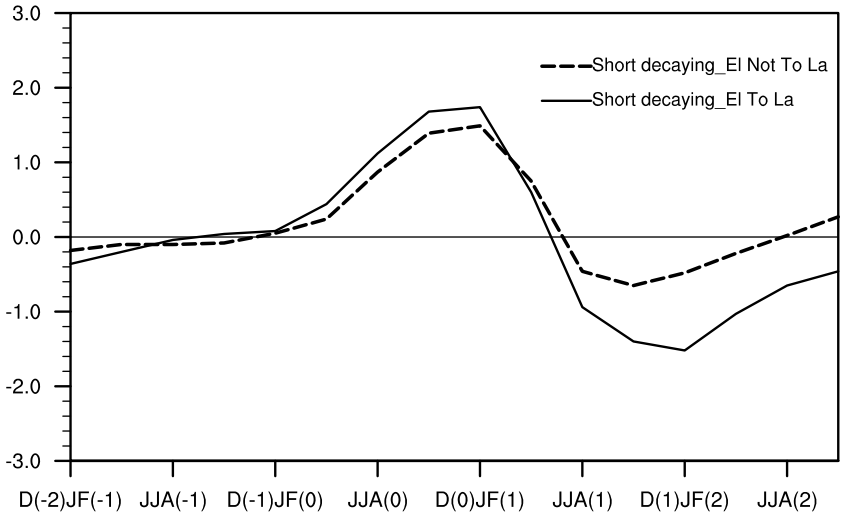

Figure 6. Composite evolutions of the Niño 3 index for the short decaying El Niño followed by La Niña events (solid line) and those not followed by La Niña events (dashed line) in the 1000-year pre-industrial simulation.

the decaying summer. Thus, both the SST anomalies in the central and eastern tropical Pacific and in the Indian Ocean contribute to the persistence of the WNPAC anomalies in the decaying summer for the short decaying El Niño events [*Terao and Kubota*, 2005]. In addition, some previous studies emphasized the role of the WNPAC anomalies in terminating El Niño events and triggering La Niña events through the anomalous easterly wind south of the WNPAC anomalies [e.g., *Weisberg and Wang*, 1997; *Wang et al.*, 1999; *Kim and Lau*, 2001; *Yun et al.*, 2009]. Our results further suggest that the short decaying of El Niño is also in favor of the WNPAC anomalies, which might imply a strong interaction between El Niño and the WNPAC anomalies in the decaying summer.

[20] For the long decaying El Niño events, the WNPAC anomalies disappear and tend to be cyclonic anomalies in JJA(1) (Figure 4f). These cyclonic circulation anomalies might be the response to the positive SST anomalies in the central and eastern tropical Pacific, even though the weak positive SST anomalies in the Indian Ocean have some roles in the WNPAC anomalies. The effects of SST anomalies in the central and eastern Pacific overwhelm those in the Indian Ocean, and induce the cyclonic circulation anomalies over the WNP.

[21] In short, the positive SST anomaly in the Indian Ocean and negative SST anomaly in the central and eastern tropical Pacific work constructively for the short decaying cases, while the positive SST anomalies over both regions work destructively for the long decaying cases. However, we could not quantitatively separate the roles of SST anomalies in the Indian Ocean and in the central and eastern tropical Pacific. Thus, the present results indicate that the different configurations of SST anomalies in the tropical Pacific and in the Indian Ocean lead to different circulation anomalies over the WNP.

3.2. Impacts of the Transition of El Niño Decaying Phases

[22] The negative SST anomalies in the central and eastern tropical Pacific in JJA(1) for the short decaying cases are more likely to be the growing phase of La Niña events. To illustrate the effects of El Niño transition, the 84 short decaying El Niño events are further divided into two categories: 45 El Niño cases followed by La Niña events in D(1)JF(2) by the criterion of the D(1)JF(2) Niño 3 index being less than −1.0 standard deviation; and other 39 El Niño cases not followed by La Niña events. The seasonal evolution of these two kinds of short decaying El Niño events is shown in Figure 6. The strength in the mature winter is slightly stronger for the El Niño with La Niña cases than that for the El Niño without La Niña cases, and they both decline in JJA(1). After JJA(1), they both have negative SST anomalies, but these signals are much weaker and recover to normal in the following year for the cases without La Niña. For the cases with La Niña, the decaying phase of El Niño is just the growing phase of the next La Niña event.

[23] The role of El Niño transition is indicated by the stronger WNPAC anomalies in JJA(1) for the El Niño followed by La Niña cases in Figure 7c. The El Niño decaying summer behaves as the La Niña growing summer, which is associated with the development of the WNPAC anomalies. As a result, the phase transition of El Niño decaying to La Niña developing leads to strong impacts of ENSO on the WNP summer anomalies. For the El Niño without La Niña type, the WNPAC anomalies in JJA(1) are much weaker. Thus, the persistence of the WNPAC anomalies related to the short decaying cases in JJA(1) shown in Figure 4c is mainly contributed to by the El Niño cases followed by La Niña, in comparison with those not followed by La Niña.

[24] Figure 8 shows the SST anomalies associated with these two categories of El Niño events. In D(0)JF(1), the SST anomalies over the Indian Ocean are stronger for the El Niño with La Niña cases (value of 0.46) than those for the El Niño without La Niña cases (value of 0.37). This further indicates that the positive Indian Ocean SST anomalies in the mature winter not only lead to the short decaying phase of El Niño, but also favor the phase transition of El Niño decaying to La Niña developing, which is consistent with *Kug and Kang* [2006]. Thus, the intensity of SST anomalies over the Indian Ocean can be treated as a precursor to the transition of the El Niño decaying phase, and therefore the strength of the WNPAC

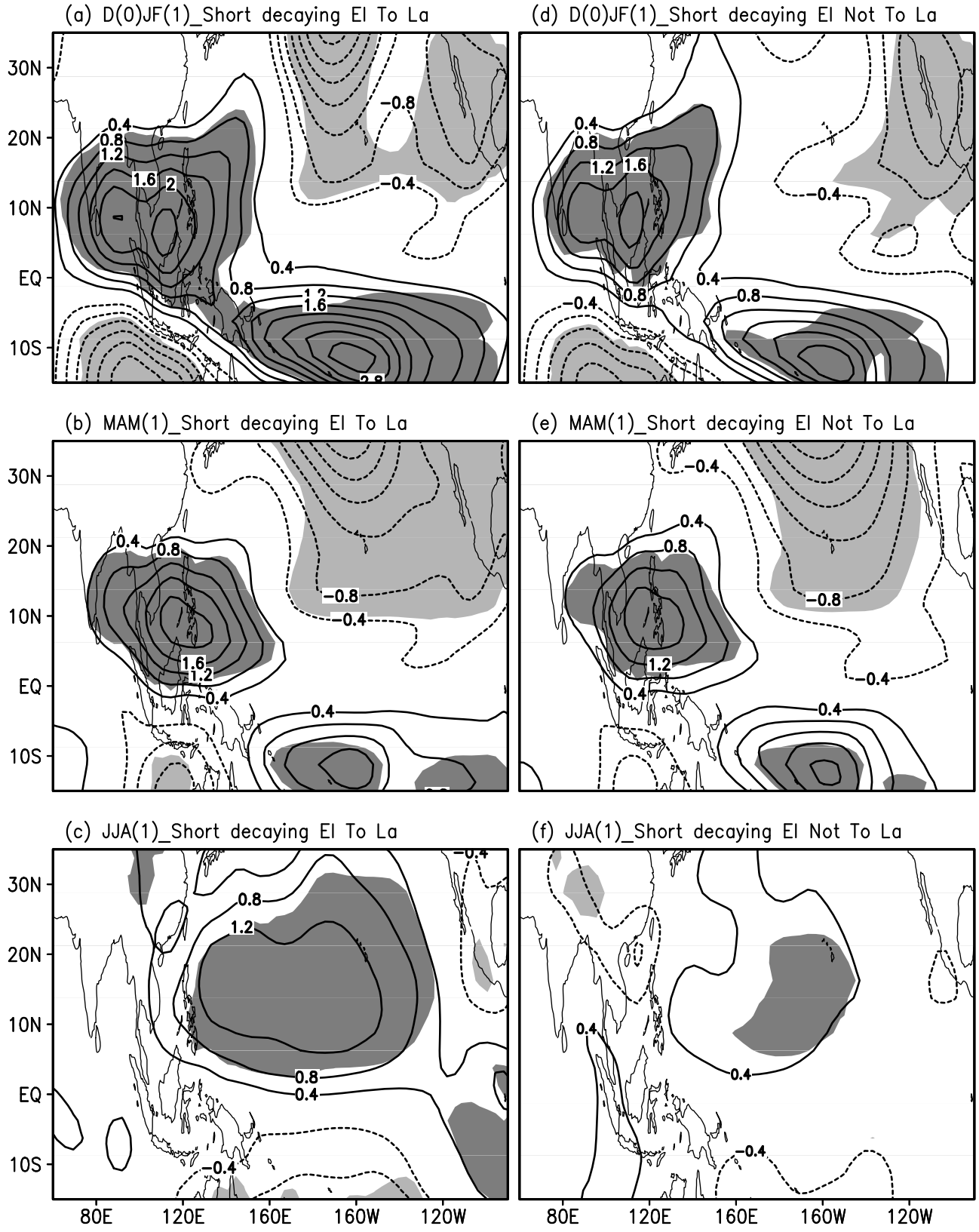

Figure 7. Composite 850-hPa stream function anomalies (unit: 10^6 m^2 s^{-1}) for (a–c) the short decaying El Niño followed by La Niña events and (d–f) those not followed by La Niña events from El Niño peak winter D(0)JF(1) to the decaying summer JJA(1). Shading indicates the region where the differences are significant at the 95% confidence level by *t*-test.

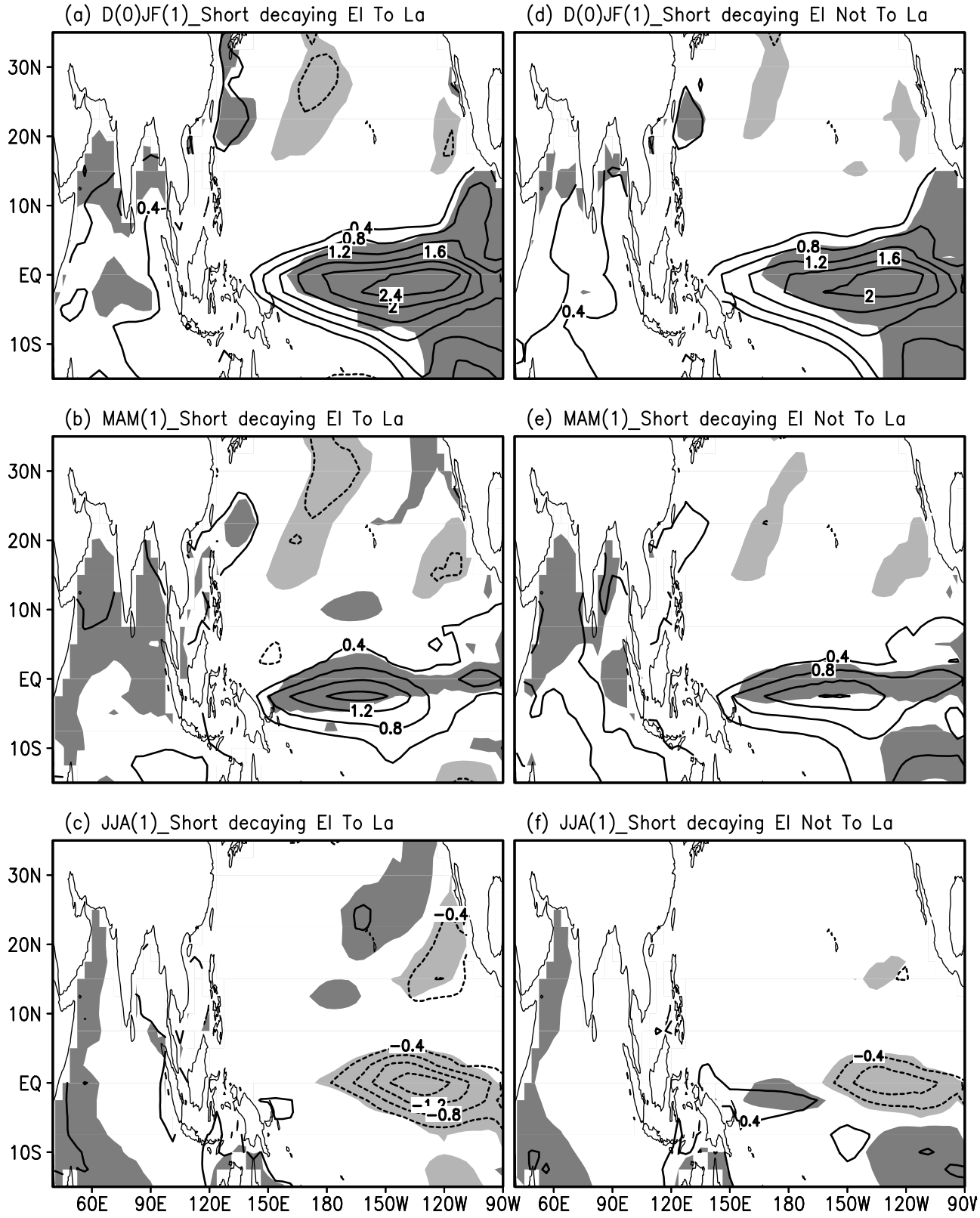

Figure 8. As in Figure 7, but for SST anomalies (units: °C).

anomalies. In JJA(1), the Indian Ocean SST anomalies are similar between the two categories, but the negative SST anomalies in the central and eastern tropical Pacific are stronger for the El Niño with La Niña cases (Figures 8c and 8f). This implies that the strong negative SST anomalies in this region might also contribute to the enhancement of the WNPAC anomalies associated with the short El Niño decaying cases followed by La Niña events.

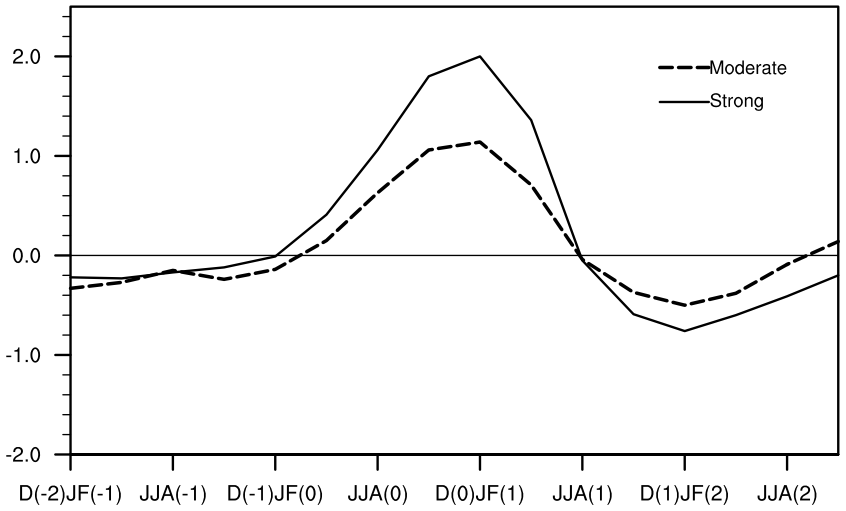

Figure 9. Composite evolution of the Niño 3 index for the strong El Niño events (solid line) and the moderate ones (dashed line) in the 1000-year pre-industrial simulation. The strong (moderate) El Niño events are defined as the Niño 3 index in the decaying summer JJA(1) being within 0.7 standard deviations and meanwhile the wintertime D(0)JF(1) Niño 3 index being greater (less) than 1.4 standard deviations.

[25] The negative SST anomalies shown in Figures 8c and 8f are more like the La Niña conditions. However, *Zhang et al.* [1996] indicated that there is no close relationship between the WNP circulation anomalies and La Niña events. To illustrate this difference, the circulation and SST anomalies associated with the La Niña cases (selected according to the DJF Niño 3 index) are further analyzed (figures not shown). We found that both for the observed and model results, a WNP anticyclonic anomaly is significant in the La Niña developing summer, but is very weak in the decaying summer. There are negative SST anomalies in the central and eastern tropical Pacific and positive SST anomalies in the Indian Ocean during the La Niña developing summer, while there are negative SSTs in both regions during the decaying summer. These results further indicate that the SST anomalies in the tropical Pacific, as well as those in the Indian Ocean, both affect the WNP circulation anomalies. The difference with *Zhang et al.* [1996] might - results from difference in analyzing periods. Our work focused on summer associated with ENSO cycles, while *Zhang et al.* [1996] focused on the whole La Niña periods.

4. Roles of the Intensity of El Niño in the Relationship Between El Niño and WNP Summer Climate

[26] In this Section, we investigate the roles of the intensity of El Niño events in D(0)JF(1) in influencing the WNPAC anomalies in JJA(1), by comparing the impacts of strong and moderate El Niño events. The strong (moderate) El Niño events are defined by the wintertime Niño 3 index anomaly being greater than 1.4 (greater than 1.0 but less than 1.4) standard deviation. Since a strong El Niño usually accompanies a the short decaying phase in this model [*Li et al.*, 2007], we attempt to exclude the effects of the El Niño decaying phase in order to focus on the impacts of El Niño strength. For this purpose, the Niño 3 index anomalies in the decaying summer JJA(1) are limited to be within 0.7 standard deviations (higher than −0.7 standard deviations and lower than 0.7 standard deviations) among the 152 El Niño cases. Actually, the approach of fixing the intensity of the JJA(1) Niño 3 index within a small range is quite similar to fixing the decaying time of El Niño within a small range of time around JJA(1). Thus, this criterion filters out the El Niño cases with very long or very short decaying phases. Under these criteria, 32 strong and 37 moderate El Niño cases are chosen. The main conclusions drawn in this Section do not change by using the thresholds of 0.3 or 0.5 instead of 0.7 standard deviations.

[27] The seasonal evolution of strong and moderate El Niño is shown in Figure 9. The development and decaying phases of the two categories of El Niño are similar. This means that the criterion we used here to distinguish the strong events with moderate ones, and meanwhile to remove the impacts of the decaying phase, is efficient. The intensity of the Niño 3 index for the strong events in the mature winter D(0)JF(1) increases by about 67% compared with the moderate ones (from 1.2 to 2.0°C). The standard deviations among the 32 strong events and 37 moderate ones are 0.55 and 0.13°C, respectively. This indicates that in comparison with the spread of the El Niño strength in each category, the difference between the two categories is remarkable.

[28] Figure 10 shows the 850-hPa stream function anomalies related to the strong and moderate El Niño events. In comparison with the moderate cases, the strength of WNPAC anomalies for the strong events is roughly twice that of the moderate cases in both D(0)JF(1) and MAM(1), consistent with the change in the Niño 3 index. During JJA(1), the strength of WNPAC anomalies is also stronger for the strong events than that for the moderate ones, even though the significant center of the circulation anomalies shifts eastward to the east of the dateline for both the categories of El Niño events. Thus, the El Niño intensity plays a role in affecting the WNPAC anomalies, with the strong wintertime El Niño inducing the strong WNPAC anomalies in the decaying summer.

[29] The spatial distributions of composite seasonal evolution of SST anomalies related to strong and moderate El Niño are similar, but their intensity is much stronger for

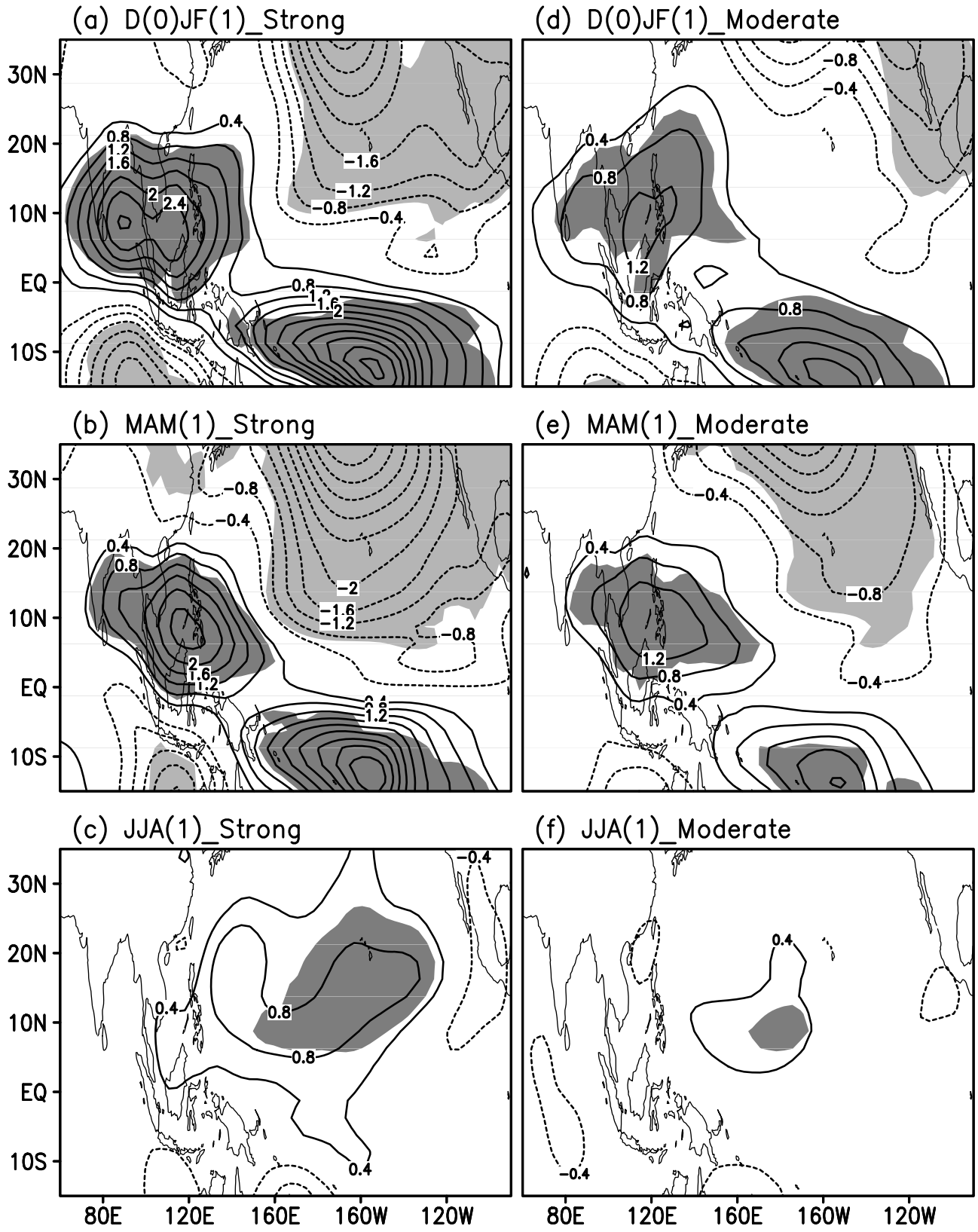

Figure 10. Composite 850-hPa stream function anomalies (units: 10^6 m^2 s^{-1}) for (a–c) the strong El Niño events and (d–f) the moderate ones from El Niño peak winter D(0)JF(1) to the decaying summer JJA(1). Shading indicates the region where the differences are significant at the 95% confidence level by *t*-test.

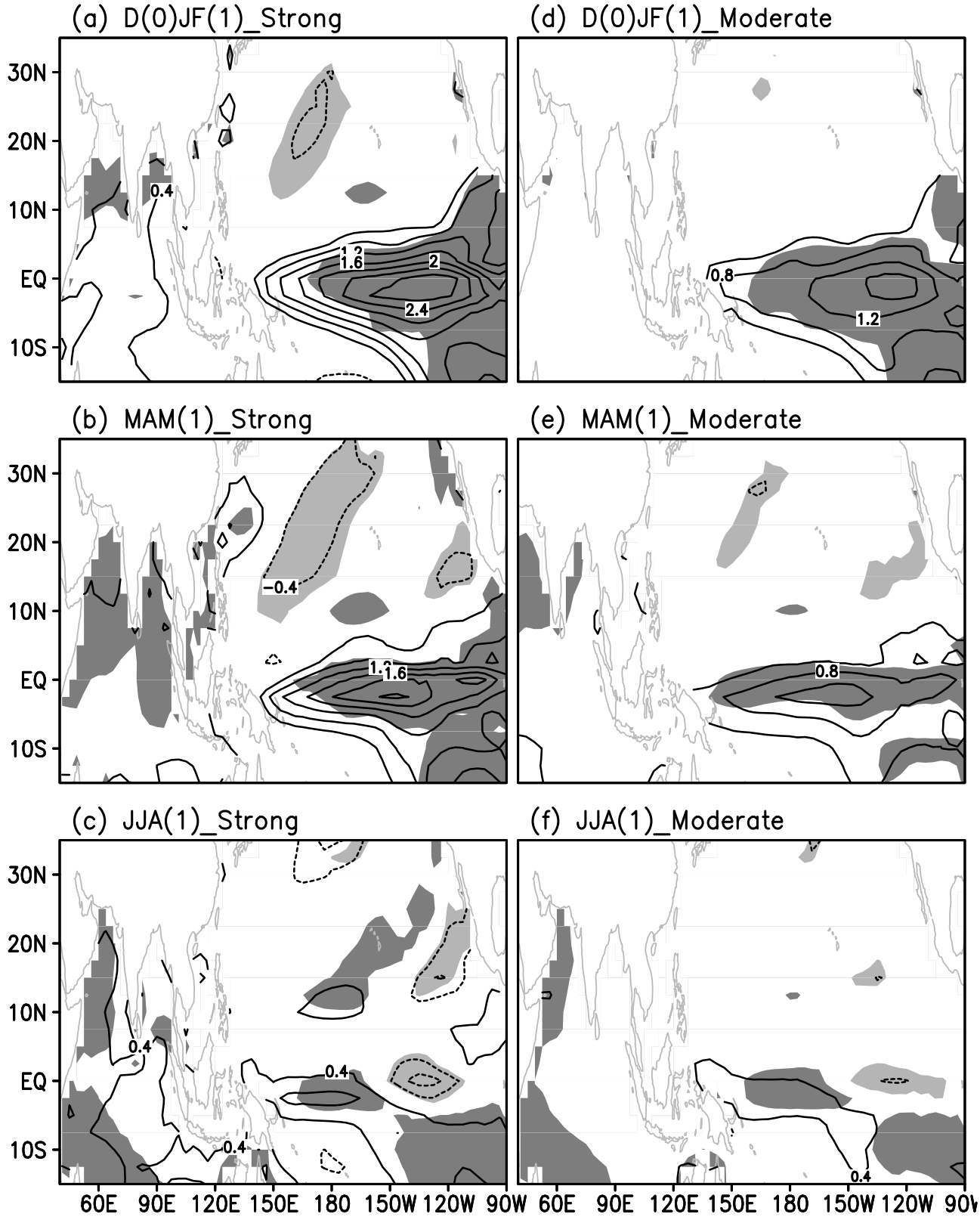

Figure 11. As in Figure 10, but for SST anomalies (unit: °C).

strong cases (Figure 11). Particularly in JJA(1), the SST anomalies in the central and eastern tropical Pacific decline to slightly positive ones in the central Pacific and negative ones in the eastern Pacific, and the positive SST anomalies are maintained in the Indian Ocean. Since the SST anomalies in the eastern tropical Pacific are both very weak for the strong and moderate cases, the stronger positive Indian Ocean SST anomalies for the strong El Niño events contribute to the

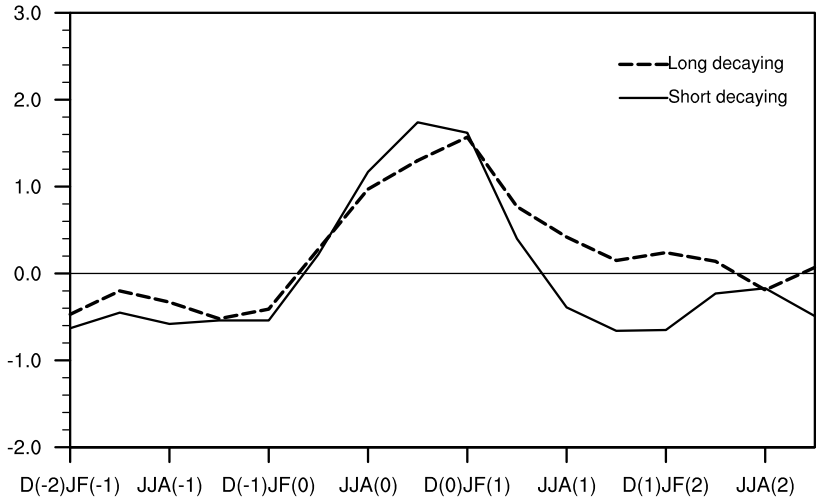

Figure 12. Composite evolution of the Niño 3 index for the short decaying El Niño events (solid line) and for the long decaying ones (dashed line) in observations. The short (long) decaying El Niño events are defined by the Niño 3 index in the decaying summer JJA(1) being less (greater) than 0°C.

enhancement of the WNPAC anomalies shown in Figure 10c, which is consistent with previous studies [*Watanabe and Jin*, 2002; *Terao and Kubota*, 2005; *Yang et al.*, 2007; *Li et al.*, 2008; *Ding et al.*, 2010; *Xie et al.*, 2009].

[30] To assess the relative roles of decaying phases and wintertime intensity of El Niño events, we further compare the categories of strong and moderate cases followed by short and long decaying phases respectively and the categories of short and long decaying cases accompanied by strong and moderate intensity respectively (figures not shown). The results indicate that the differences between the strong and moderate cases (no matter if followed by short or long decaying phases) are weaker than those between the short and long decaying cases (no matter if accompanied by strong or moderate intensity). This suggests that the duration of El Niño decaying phases has remarkable impacts on the WNPAC anomalies and the wintertime intensity of El Niño plays a secondary role.

[31] The present results emphasize that the El Niño decaying phase plays an important role in the persistence of WNPAC anomalies in the decaying summer in addition to the wintertime El Niño strength. The results given by *Li et al.* [2007] that the strong El Niño events are in favor of strong WNPAC anomalies in the decaying summer, is essentially due to the fact that strong El Niño events tend to be followed by short decaying phases and transformation to La Niña events. Therefore, in their study, the effects of decaying phases and the intensity of El Niño are mingled. The present results indicate that it is necessary to separate the roles of the El Niño decaying phase and the wintertime intensity in order to better understand better the mechanisms responsible for the impacts of decaying El Niño events on the WNPAC anomalies.

5. Observed Evidence About the Impacts of El Niño Decaying Phases

[32] The strong influence of El Niño decaying phases on the WNPAC anomalies was also investigated in observational data. The 11 El Niño events in Figure 1 are divided into five short decaying and six long decaying cases, according to the strength of the Niño 3 index in JJA(1) being less or greater than 0°C. The years 1951/52, 1965/66, 1972/73, 1994/95 and 1997/98 are defined as the short decaying El Niño events, and the years 1957/58, 1976/77, 1982/83, 1986/87, 1991/92 and 2002/03 are the long decaying cases. It should be noted that the case of 1986/87 is a special one in that it has the mature phase in summer, rather than winter, so we exclude it from the long decaying cases in the following.

[33] The composite seasonal evolution of the two classes of El Niño events is shown in Figure 12. Both the short and long decaying cases share the similar developing phases and intensities in the mature winter, but the decaying durations are different. The averaged Niño 3 index in JJA(1) is −0.39°C for the short decaying events, much lower than that for the long decaying ones (0.42°C).

[34] Figure 13 shows the impacts of the different El Niño decaying phases on the WNPAC anomalies in observations. The WNPAC anomalies are strong in D(0)JF(1) and decline rapidly in MAM(1) for both the short and long decaying El Niño cases. However, for the short decaying cases, the WNPAC anomalies are reinforced again during the decaying summer (Figure 13c), which are in contrast with the insignificant circulation anomalies over the WNP for the long decaying events in JJA(1) (Figure 13f). These pronounced differences of the WNPAC anomalies in JJA(1) associated with different categories of El Niño events indicate a stronger relationship between the short decaying El Niño and the WNP summer anomalies, which are consistent with the model results (Figure 4). In addition, a pair of cyclonic circulation anomalies located in the eastern Pacific corresponds to the evolution of El Niño events. The strength of the pair of cyclonic circulation anomalies is stronger in D(0)JF(1) and MAM(1) for the long decaying events than those for the short decaying ones. The stronger westerly anomalies induced by the pair of cyclone anomalies favor the positive SST anomalies maintaining in the central and eastern tropical Pacific, which lead to a long decaying phase of El Niño.

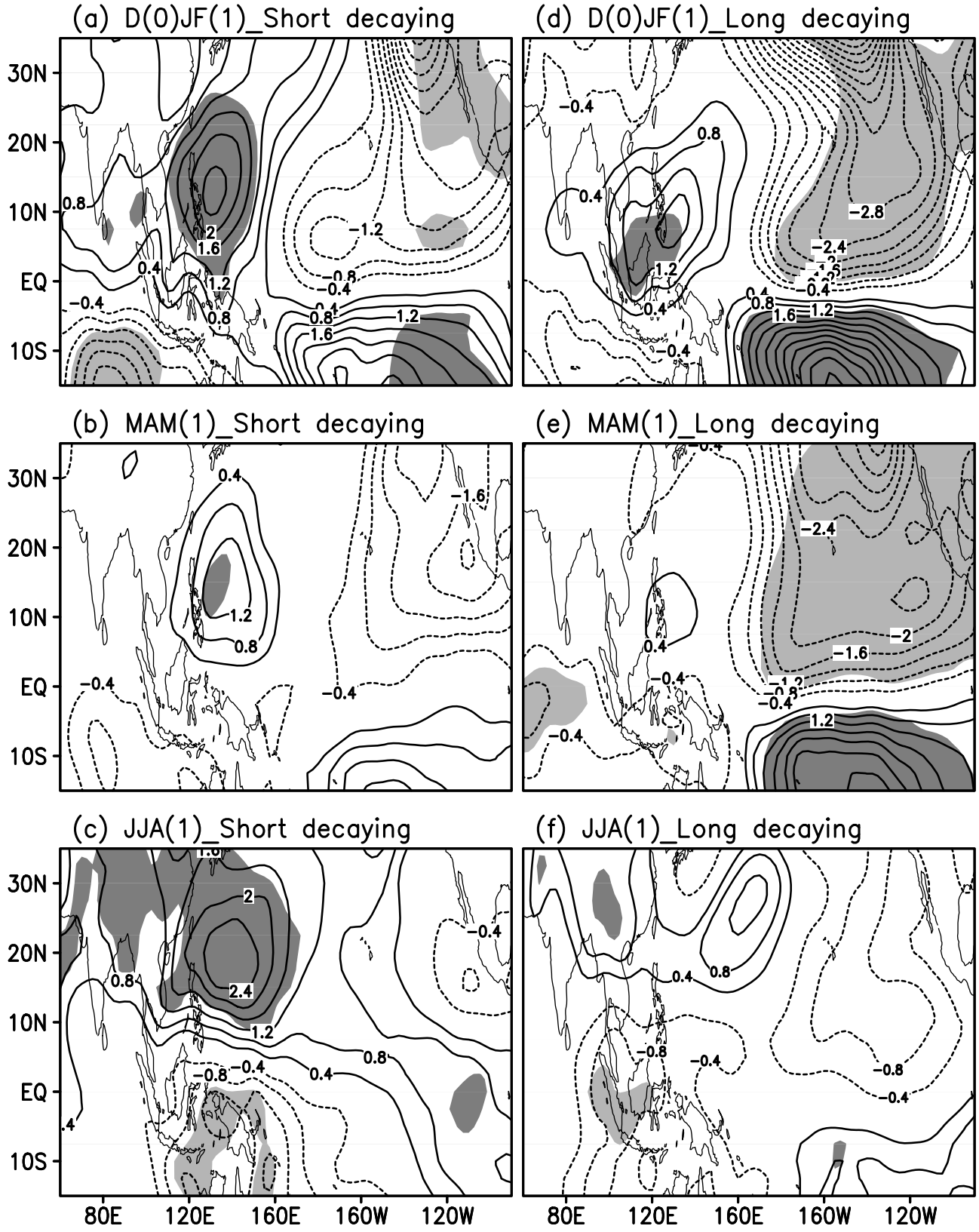

Figure 13. Composite 850-hPa stream function anomalies (units: 10^6 m^2 s^{-1}) for the (a–c) short decaying El Niño events and (d–f) long decaying ones in observations from El Niño peak winter D(0)JF(1) to the decaying summer JJA(1). Shading indicates the region where the differences between short (long) decaying cases and normal cases are significant at the 95% confidence level by *t*-test.

The features of the pair of cyclone anomalies in the eastern Pacific are also consistent with the model results (Figure 4).

[35] For the short decaying El Niño events, the WNPAC anomalies in JJA(1) are stronger than those in MAM(1) (Figures 13b and 13c), which is inconsistent with the model results (Figures 4b and 4c). This might be due to some uncertainties in the composite results induced by a small number of events in observations. There are great differences in stream function and SST anomalies among the five short decaying cases. Some descriptions about the circulation and SST anomalies for these cases are given below, without figures being shown. The weakness of composite WNPAC anomalies in MAM(1) relative to those in JJA(1) is mainly caused by the 1965/66 and 1994/95 cases. In these two cases, over the WNP, there are cyclonic anomalies in MAM(1), associated with positive SST anomalies in the central tropical Pacific, and anticyclonic anomalies in JJA(1), without significant SST anomalies in the central tropical Pacific.

[36] Similarly, the uncertainty of the composite observed results induced by the small number of samples in observations prompts the differences between the model and observational results (Figures 4c and 13c). Among the five short decaying cases in observations, for three cases (1951/52, 1965/66 and 1972/73) there are WNPAC anomalies extending from the WNP to the central and eastern Pacific, while for the other two cases (1994/95 and 1997/98), the WNPAC anomalies are limited to the west of the dateline and cyclonic anomalies are located in the eastern Pacific (figures not shown). The WNPAC anomalies associated with the short decaying cases in the model (Figure 4c) resemble well the observed ones for the former three cases, and show a discrepancy with the latter two cases over the eastern Pacific. Thus, the differences in the circulation anomalies between Figure 4c (model) and Figure 13c (observations) might not be necessary to indicate that the model fails in capturing the ENSO-related circulation anomalies over the eastern Pacific.

[37] The structures of circulation anomalies associated with the short and long decaying El Niño events are shown by the 850-hPa wind anomalies in Figure 14, which further illustrates that the short decaying cases are related to the stronger WNPAC anomalies in JJA(1). For the long decaying cases, the westerly anomalies in the northeastern subtropical Pacific are associated with the wind anomalies in the higher latitudes instead of those in the tropical region during MAM(1) and JJA(1). From the details of circulation anomalies associated with El Niño shown by the 850-hPa wind anomalies in Figure 14, we further conclude that the short decaying phases of El Niño are important to the WNPAC anomalies. In observations, we do not divide the short decaying El Niño into 'followed by' or 'not followed by' La Niña types, because of the small number of samples. The anticyclonic circulation anomalies over the WNP shown as Figure 14c are very similar with a typical anomalous wind pattern associated with the growing phase of La Niña. This implies a role of El Niño transition in the WNPAC anomalies for the short decaying cases in observations, being consistent with the model results.

[38] The SST anomalies associated with the different El Niño decaying phases in observations are illustrated in Figure 15. In D(0)JF(1), the positive SST anomalies over the Indian Ocean are stronger for the short decaying cases than those for the long decaying cases, especially in the western Indian Ocean. These Indian Ocean SST anomalies contribute to the transition of an El Niño decaying phase to a La Niña developing phase [*Kug and Kang*, 2006], and the phase transition is in favor of the enhancement of WNPAC anomalies in the El Niño decaying summer (Figure 13c), which supports the model results.

[39] In JJA(1), the composite SST anomalies in observations bear some similarities to those in the model results, especially for the long decaying cases. However, the magnitudes of SST anomalies in both the Indian Ocean and tropical Pacific are weak for the short decaying cases, while they are slightly stronger for the long decaying cases in observations in comparison with the model results (Figure 5). It is worth pointing out that there are some uncertainties in the observational composites due to a small number of samples and therefore it is difficult to disentangle whether these differences between observational and model results reflect a model deficiency or uncertainty due to an insufficient number of samples in observations. For the long decaying cases, the roles of the positive SST anomalies in the Indian Ocean and in the central and eastern tropical Pacific work destructively and induce weak WNP circulation anomalies, which are similar to those discussed in the model simulation (Figure 5f).

6. Discussion and Conclusions

[40] The influence of El Niño behavior on the relationship between El Niño and the WNP summer climate has been investigated by using a 1000-year pre-industrial simulation. The relationship is characterized as the strength of the WNPAC anomalies in the El Niño decaying summer. The roles of El Niño decaying phase and the El Niño intensity in inducing the WNPAC anomalies have been illustrated respectively. The results suggest that the transition of decaying phases is another important factor influencing the WNPAC anomalies in the decaying summer in addition to El Niño intensity. The short decaying phases lead to an enhancement of the WNPAC anomalies, and among these short decaying events, the strong WNPAC anomalies are contributed to mainly by those El Niño cases that are followed by La Niña. On the contrary, the long decaying phases are related to the weak WNP circulation anomalies in the El Niño decaying summer. These model results are basically supported by observed evidence, although the number of El Niño cases is limited in observations.

[41] The present results suggest that the strength of SST anomalies over the Indian Ocean in the mature winter D(0)JF(1) might play an important role in leading to different lengths of El Niño decaying phases. The D(0)JF(1) SST anomalies in the Indian Ocean are significantly positive (regional averaged value of 0.42°C) for the short decaying cases, but they are insignificant and very weak (0.22°C), although positive, for the long decaying cases. On the other hand, the D(0)JF(1) SST anomalies in the eastern tropical Pacific are similar between the short and long decaying cases. The wintertime positive SST anomalies in the Indian Ocean generate the easterly anomaly extending to the western and central equatorial Pacific in the subsequent spring and summer, which leads to a decline of positive SST anomalies in the eastern

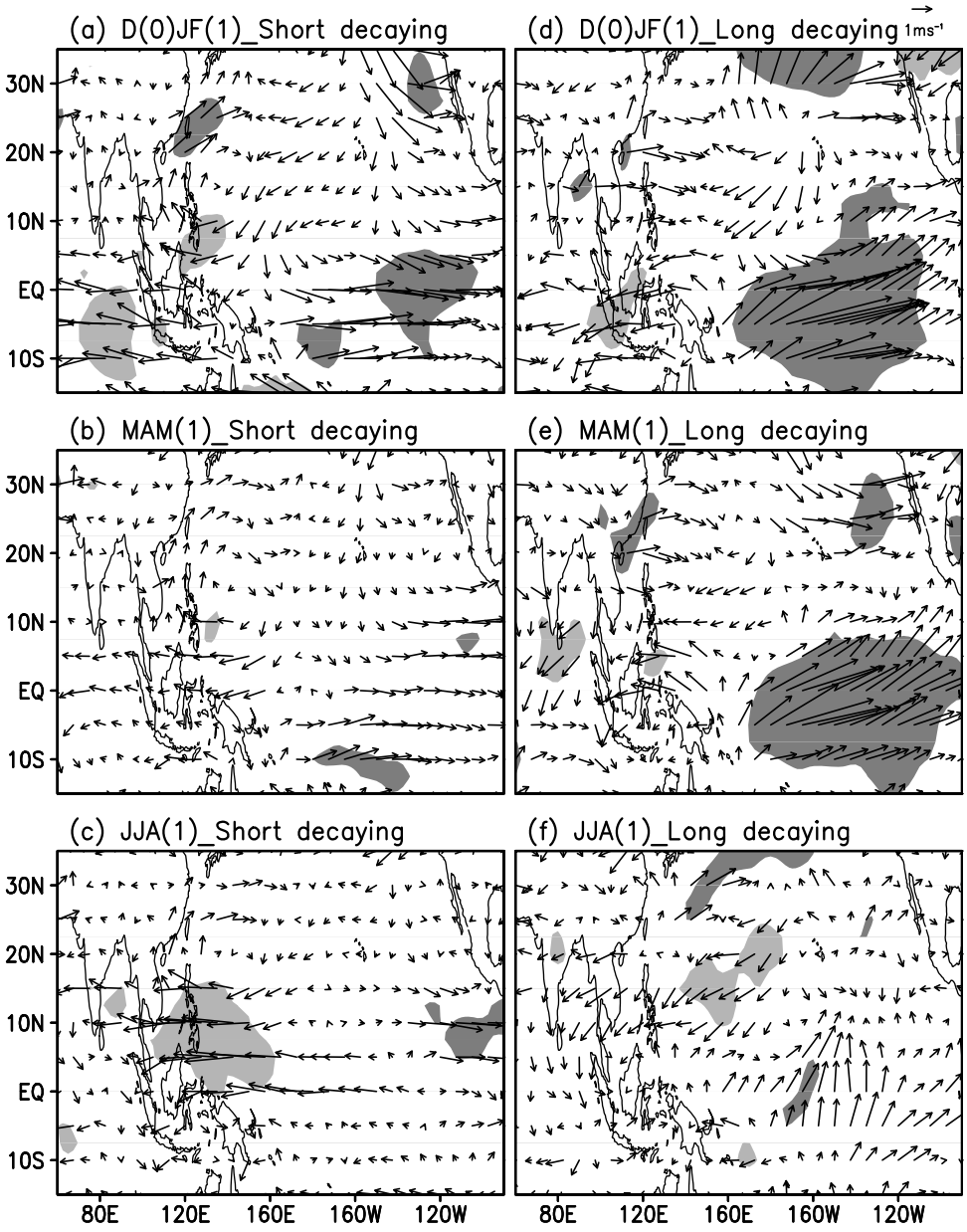

Figure 14. As in Figure 13, but for 850-hPa wind anomalies (units: m s^{-1}).

tropical Pacific and results in a short decaying of El Niño. Therefore, the strength of the positive D(0)JF(1) SST anomalies in the Indian Ocean tends to be a precursor to the different decaying phases of El Niño.

[42] During the El Niño decaying summer JJA(1), the configurations of SST anomalies in the Indian Ocean and in the central and eastern tropical Pacific lead to the difference in the strength of the WNPAC anomalies. For the short decaying cases, both positive SST anomalies in the Indian Ocean and the negative SST anomalies in the central and eastern tropical Pacific work constructively and contribute to the persistence of significant WNPAC anomalies. For the long decaying phase, though the WNPAC anomalies can be induced by the positive SST anomalies in the Indian Ocean, they are offset by the role of positive SST anomalies in the central and eastern tropical Pacific, leading to weak circulation anomalies over the WNP.

[43] The impacts of El Niño intensity on the WNPAC anomalies in the El Niño decaying summer have also been illustrated in our study. The El Niño intensity also plays a role in the WNPAC anomalies during the decaying summer. Considering strong El Niño events are often followed by a short decaying phase, we defined the strong and moderate events both decline in the summer JJA(1), in order to distinguish the impacts of El Niño intensity and decaying phase. Both the strong and moderate El Niño events induce the WNPAC anomalies in the decaying summer, but the

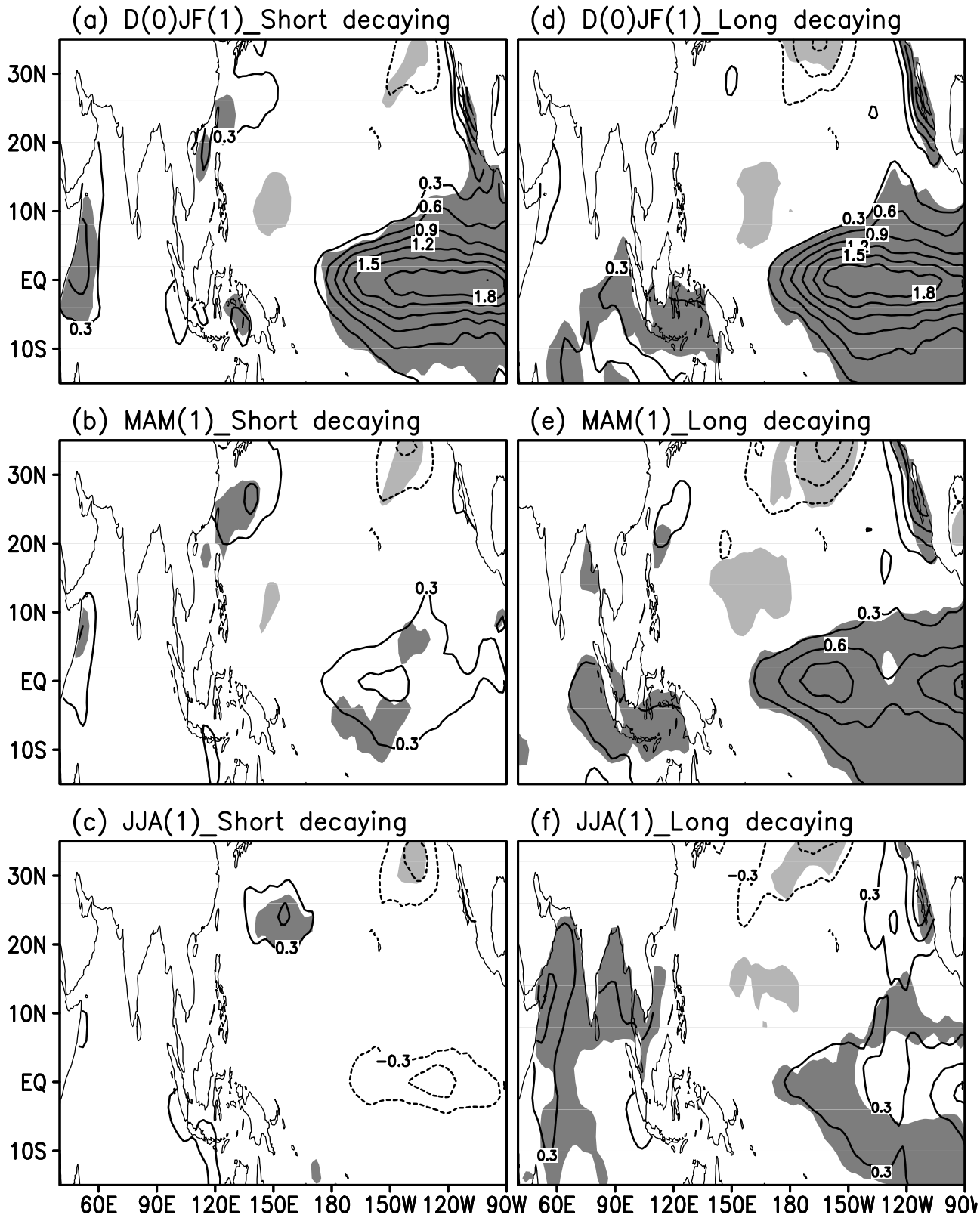

Figure 15. As in Figure 13, but for SST anomalies (units: °C).

strength of the WNPAC anomalies are stronger for the strong events, which is consistent with previous studies.

[44] The model and observed results indicate that the transition of El Niño decaying phases is important for the impacts of El Niño on the WNP summer anomalies. Thus, attention should be paid not only to the strength of El Niño but also to the El Niño decaying phases for the prediction of the WNP summer climate.

[45] **Acknowledgments.** This work was supported by the National Research Foundation (NRF) of Korea Grand funded by the Korea government (MEST) (2010–0028715), and also supported by the Ministry of Finance of China (grant GYHY201006021). B. Dong was supported by the U.K. National Centre for Atmospheric Science-Climate (NCAS-Climate).

References

Annamalai, H., S.-P. Xie, J. P. McCreary, and R. Murtugudde (2005), Impact of Indian Ocean sea surface temperature on developing El Niño, *J. Clim.*, *18*, 302–319, doi:10.1175/JCLI-3268.1.

Annamalai, H., S. Kida, and J. Hafner (2010), Potential impact of the tropical Indian Ocean-Indonesian seas on El Niño characteristic, *J. Clim.*, *23*, 3933–3952, doi:10.1175/2010JCLI3396.1.

Boo, K.-O., G.-H. Lim, and K.-Y. Kim (2004), On the low-level circulation over the western North Pacific in relation with the duration of El Niño, *Geophys. Res. Lett.*, *31*, L10202, doi:10.1029/2004GL019418.

Chang, C.-P., Y. Zhang, and T. Li (2000), Interannual and interdecadal variations of the East Asian summer monsoon and tropical Pacific SSTs. Part I: Roles of the subtropical ridge, *J. Clim.*, *13*, 4310–4325, doi:10.1175/1520-0442(2000)013<4310:IAIVOT>2.0.CO;2.

Chou, C., J.-Y. Tu, and J.-Y. Yu (2003), Interannual variability of the western North Pacific summer monsoon: Differences between ENSO and non-ENSO years, *J. Clim.*, *16*, 2275–2287, doi:10.1175/2761.1.

Chou, C., L.-F. Huang, J.-Y. Tu, L. Tseng, and Y.-C. Hsueh (2009), El Niño impacts on precipitation in the western North Pacific–East Asian sector, *J. Clim.*, *22*, 2039–2057, doi:10.1175/2008JCLI2649.1.

Ding, R., K.-J. Ha, and J. Li (2010), Interdecadal shift in the relationship between the East Asian summer monsoon and the tropical Indian Ocean, *Clim. Dyn.*, *34*, 1059–1071, doi:10.1007/s00382-009-0555-2.

Gordon, C., C. Cooper, C. A. Senior, H. Banks, J. M. Gregory, T. C. Johns, J. F. B. Mitchell, and R. A. Wood (2000), The simulation of SST, sea ice extents and ocean heat transports in a version of the Hadley Centre coupled model without flux adjustments, *Clim. Dyn.*, *16*, 147–168, doi:10.1007/s003820050010.

Hu, K.-M., and G. Huang (2010), The formation of precipitation anomaly patterns during the developing and decaying phases of ENSO, *Atmos. Oceanic Sci. Lett.*, *3*, 25–30.

Kalnay, E., et al. (1996), The NECP-NCAR 40-year reanalysis project, *Bull. Am. Meteorol. Soc.*, *77*, 437–471, doi:10.1175/1520-0477(1996)077<0437:TNYRP>2.0.CO;2.

Kim, K. M., and K. M. Lau (2001), Dynamics of monsoon-induced biennial variability in ENSO, *Geophys. Res. Lett.*, *28*, 315–318, doi:10.1029/2000GL012465.

Kug, J.-S., and I.-S. Kang (2006), Interactive feedback between ENSO and the Indian Ocean, *J. Clim.*, *19*, 1784–1801, doi:10.1175/JCLI3660.1.

Lau, N. C., and M. J. Nath (2000), Impacts of ENSO on variability of the Asian-Australian monsoons as simulated in GCM experiments, *J. Clim.*, *13*, 4287–4309, doi:10.1175/1520-0442(2000)013<4287:IOEOTV>2.0.CO;2.

Lau, N. C., and M. J. Nath (2003), Atmosphere-ocean variations in the Indo-Pacific sector during ENSO episodes, *J. Clim.*, *16*, 3–20, doi:10.1175/1520-0442(2003)016<0003:AOVITI>2.0.CO;2.

Li, S., J. Lu, G. Huang, and K. Hu (2008), Tropical Indian Ocean basin warming and East Asian summer monsoon: A multiple AGCM study, *J. Clim.*, *21*, 6080–6088, doi:10.1175/2008JCLI2433.1.

Li, Y., R. Lu, and B. Dong (2007), The ENSO–Asian monsoon interaction in a coupled ocean–atmosphere GCM, *J. Clim.*, *20*, 5164–5177, doi:10.1175/JCLI4289.1.

Lin, Z., and R. Lu (2009), The ENSO's effect on eastern China rainfall in the following early summer, *Adv. Atmos. Sci.*, *26*, 333–342, doi:10.1007/s00376-009-0333-4.

Nitta, T. (1987), Convective activity in the tropical western Pacific and their impact on the Northern Hemisphere summer circulation, *J. Meteorol. Soc. Jpn.*, *65*, 373–390.

Ohba, M., and H. Ueda (2007), An impact of SST anomalies in the Indian Ocean in acceleration of the El Niño to La Niña transition, *J. Meteorol. Soc. Jpn.*, *85*, 335–348, doi:10.2151/jmsj.85.335.

Pope, V. D., M. L. Gallani, P. R. Rowntree, and R. A. Stratton (2000), The impact of new physical parameterizations in the Hadley Centre climate model: HadAM3, *Clim. Dyn.*, *16*, 123–146, doi:10.1007/s003820050009.

Smith, T. M., and R. W. Reynolds (2004), Improved extended reconstruction of SST (1854–1997), *J. Clim.*, *17*, 2466–2477, doi:10.1175/1520-0442(2004)017<2466:IEROS>2.0.CO;2.

Terao, T., and T. Kubota (2005), East-west SST contrast over the tropical oceans and the post El Niño western North Pacific summer monsoon, *Geophys. Res. Lett.*, *32*, L15706, doi:10.1029/2005GL023010.

Ueda, H., and J. Matsumoto (2000), A possible triggering process of east-west asymmetric anomalies over the Indian Ocean in relation to 1997/98 El Nino, *J. Meteorol. Soc. Jpn.*, *78*, 803–818.

Wang, B., R. Wu, and T. Li (2003), Atmosphere–warm ocean interaction and its impacts on Asian–Australian monsoon variability, *J. Clim.*, *16*, 1195–1211, doi:10.1175/1520-0442(2003)16<1195:AOIAII>2.0.CO;2.

Wang, B., J. Yang, T. Zhou, and B. Wang (2008), Interdecadal changes in the major modes of Asian–Australian monsoon variability: Strengthening relationship with ENSO since the late 1970s, *J. Clim.*, *21*, 1771–1789, doi:10.1175/2007JCLI1981.1.

Wang, C., R. H. Weisberg, and J. I. Virmani (1999), Western Pacific interannual variability associated with El Niño-Southern Oscillation, *J. Geophys. Res.*, *104*, 5131–5149, doi:10.1029/1998JC900090.

Watanabe, M., and F. Jin (2002), Role of Indian Ocean warming in the development of Philippine Sea anticyclone during ENSO, *Geophys. Res. Lett.*, *29*(10), 1478, doi:10.1029/2001GL014318.

Weisberg, R. H., and C. Wang (1997), Slow variability in the equatorial west-central Pacific in relation to ENSO, *J. Clim.*, *10*, 1998–2017, doi:10.1175/1520-0442(1997)010<1998:SVITEW>2.0.CO;2.

Xie, S.-P., H. Annamalai, F. A. Schott, and J. P. McCreary (2002), Structure and mechanisms of South Indian Ocean climate variability, *J. Clim.*, *15*, 864–878, doi:10.1175/1520-0442(2002)015<0864:SAMOSI>2.0.CO;2.

Xie, S.-P., K. Hu, J. Hafner, H. Tokinaga, Y. Du, G. Huang, and T. Sampe (2009), Indian Ocean capacitor effect on Indo–Western Pacific climate during the summer following El Niño, *J. Clim.*, *22*, 730–747, doi:10.1175/2008JCLI2544.1.

Xue, F., and C. Liu (2008), The influence of moderate ENSO on summer rainfall in eastern China and its comparison with strong ENSO, *Chin. Sci. Bull.*, *53*, 791–800, doi:10.1007/s11434-008-0002-5.

Yang, J., Q. Liu, S.-P. Xie, Z. Liu, and L. Wu (2007), Impact of the Indian Ocean SST basin mode on the Asian summer monsoon, *Geophys. Res. Lett.*, *34*, L02708, doi:10.1029/2006GL028571.

Yun, K.-S., B. Ren, K.-J. Ha, J. Chan, and J.-G. Jhun (2009), The 30–60 day oscillation in the East Asian summer monsoon and its time-dependent association with the ENSO, *Tellus, Ser. A*, *61*, 565–578, doi:10.1111/j.1600-0870.2009.00410.x.

Zhang, R., and A. Sumi (2002), Moisture circulation over East Asia during El Niño episode in northern winter, spring and autumn, *J. Meteorol. Soc. Jpn.*, *80*, 213–227, doi:10.2151/jmsj.80.213.

Zhang, R., A. Sumi, and M. Kimoto (1996), Impact of El Niño on the East Asia Monsoon: A diagnostic study of the '86/87 and '91/92 events, *J. Meteorol. Soc. Jpn.*, *74*, 49–62.

Zhang, R., A. Sumi, and M. Kimoto (1999), A diagnostic study of the impact of El Niño on the precipitation in China, *Adv. Atmos. Sci.*, *16*, 229–241, doi:10.1007/BF02973084.